AgriVoltaics World Conference 2024

Environmental Modeling

https://doi.org/10.52825/agripv.v3i.1370

Published: 29 Apr. 2025

A Simple Approach for Clustering Common Insolation Profiles in Agrivoltaic Systems

Ganesh Pandey[1,*], Sarah Lyden[1], Evan Franklin[1], and Matthew Tom Harrison[2]

[1]School of Engineering, University of Tasmania, Hobart, Australia

[2]Tasmanian Institute of Agriculture, University of Tasmania, Launceston, Australia

*Correspondence: Ganesh Pandey, Ganesh.Pandey@utas.edu.au

Abstract. Heterogeneous insolation distribution in agrivoltaic systems (AVS) impacts plant growth beneath solar panels via shading and perturbed evapotranspiration profiles. Most agricultural systems models, meanwhile, assume uniform irradiance patterns across an entire field when simulating biomass production, meaning that they cannot readily account for spatiotemporal trade-offs between agricultural production and energy generation pertaining to AVS. We develop a simple approach for enumerating trade-offs between crop/pasture production and energy generation that accounts for spatial heterogeneity in insolation that typifies most AVS fields. First, long-term spatially explicit daily insolation profiles at the ground surface are produced for several layouts, including variations in PV panel orientations, row spacings, heights and tilt angles. A clustering technique was then applied to all insolation profiles to group them into rationally bounded cluster groups. The insolation profile of each cluster group was set as an input to a conventional point-based agricultural systems model to determine agricultural production under heterogeneous insolation profiles. The proposed approach is applied to a case study near Hobart, Australia, to determine an optimal layout that maximizes energy generation and plant growth associated with 81 AVS layouts. We find a manageable number (19 clusters) of point-based agricultural model scenarios capture much of the variance in insolation variability associated with varying AVS layouts. Compared with open fields, we show that AVS can amplify pasture growth rates during late spring and early summer. The optimal layout for our case study region enhanced land productivity by 47% while maintaining 80% of agricultural production compared with open-field agriculture.

Keywords: Agrivoltaic System (AVS), AVS Layout Optimization, Livestock-Based AVS, K-Means Clustering, Land Equivalent Ratio

1. Introduction

Agrivoltaic systems (AVS) co-locate photovoltaic (PV) electricity generation and agri-food production on the same land parcel. Previous work has shown that AVS layouts can achieve land equivalent ratios (LERs) ranging from 1.35-1.73, suggesting a 35-73% increase in land productivity compared with the conventional approach of using the same land for either PV electricity generation or agri-food production [1]. Recent advances in AVS research reveal additional benefits such as increased water-use efficiency resulting in a decrease in evapotranspiration and plant water-deficit [2], resilience of crop yield against climate change [3], income diversification for farmers [4], greenhouse gas emissions abatement [5], and promotion of animal welfare [6].

Solar panels intercept and reduce the amount of solar radiation reaching the ground, which can impact the growth of plants and consequently affect evapotranspiration and plant growth depending on genetic shade tolerance [7]. The layout of PV systems in AVS must be appropriately selected to compensate for the reduction in agricultural yield, such as by increasing row spacing, reducing solar panel density in each row, and using semi-transparent solar panels [8, 9]. Hence, an optimal AVS layout must find a suitable compromise between PV electricity generation and agricultural production [10]. The optimal configuration should also account for location-specific factors such as latitude (day length), solar radiation, and precipitation that can impact PV electricity generation and agricultural production.

Modelling or simulation-based studies provide cost-effective measures to determine the potential of AVS to generate PV electricity and biomass production, by accounting for location-specific climatic constraints. Such approaches provide an opportunity to select an optimal AVS layout for a given location and crop or pasture type, according to a pre-determined set of criteria. In this regard, conventional PV system models, such as the System Advisor Model (SAM®) [11], can be utilized to determine PV electricity production potential in AVS. However, solar panels cause spatio-temporal variation in shadows cast on the ground, and thus heterogeneous insolation distribution across the AVS site [1, 12]. The occurrence of heterogenous distribution of insolation in turn can result in non-uniform plant growth rates across the site, which poses a significant challenge in selecting an appropriate agricultural model to accurately simulate plant growth and determine agricultural yield in AVS. This is because most agricultural simulation models are typically "point-based" in nature and assume homogenous soil and climate across the entire field. Thus, they cannot readily account for spatiotemporal variation in insolation heterogeneity observed within the AVS site while determining biomass yield. We opine that robust assessment of the trade-offs between agricultural productivity and energy generation in AVS requires quantification of biomass production through spatially independent points formed by heterogeneity in insolation distribution.

Previous studies have accounted for variation in insolation in AVS compared with the open field conditions by a) assuming a constant shading factor that represents an average reduction in insolation in AVS compared with the full-sun or open-field conditions [13], b) computing time-varying diffuse and direct irradiation received at separate points in the ground within the space between two rows of solar panels (row space) and then determining average ground horizontal irradiation across the row space [14], or c) computing time-varying diffuse and direct irradiation received at separate points in the field and then individually determining irradiation reduction for each point [3, 15]. The latter two approaches capture temporal and spatial variations in insolation received by vegetation within AVS site. However, to determine the optimal AVS layout, the impact of an extensive array of PV systems layouts on PV electricity and agricultural production can be computationally expensive. In this paper we address this research gap by developing a novel method that enables efficient assessment of combined energy and agricultural production in AVS with high spatial heterogeneity via a case study with pasture produced in AVS.

2. Methods

Our approach first determines time-dependent insolation distribution observed across the ground considering direct and diffuse irradiation received at every ground position within an AVS site for any sun position at hourly-time scale. This is repeated for all known sun positions throughout the year for a given site, and for a wide variety of different AVS layouts, to produce a large array of insolation profiles, one for every layout and ground position. Since, most agricultural models simulate agricultural production at daily timescale, the generated array of insolation profiles at hourly scale are summed up to yield the daily insolation for each day of the year at each ground position and layout. Then, the daily insolation profiles at every ground position for each layout are provided as inputs to a clustering algorithm, which groups together ground positions that experience similar daily insolation profile. The clustering algorithm groups the ground positions of all AVS layouts into 'k' number of rationally bounded clusters based on the similarity of their daily insolation profile. Next, the insolation profile of each of the ‘k’ clusters is supplied as an input parameter to a point-based agricultural system model to simulate daily agricultural production at areas within the AVS field receiving this insolation distribution. Hence, by simulating agricultural production under 'k' number of heterogenous insolation conditions, pasture production for each AVS layout is determined by accounting for the area of the AVS field covered by each insolation cluster. PV electrical output for each of the AVS layouts is determined using conventional PV system models. Consequently, the electrical and agricultural productivity of each AVS layout is determined, allowing for the subsequent calculation of the LER for each layout. The optimal layout to meet a given user-defined optimization objective can then be selected. We conducted a case study to demonstrate the proposed method.

2.1 Insolation Modelling

Field surface insolation within the AVS site are calculated by modelling the PV array as a collection of parallel rows of solar panels, oriented with an azimuth angle of θ, row spacing of D and with the lower edge of each row a distance h above the ground, as illustrated in *Figure 1*. Each row consists of solar panels of length l, mounted at a fixed tilt angle of ϕ. We assume each row has a long arrangement of side-by-side connected monofacial (opaque) solar panels; thus, there is no border effect on insolation distribution within the AVS site.

At any location, insolation received at any ground position depends on diffuse and direct irradiation, which are both influenced by shading caused by solar panels. For any given ground position and sun position, direct irradiation will either be masked by one or more rows of solar panels or otherwise will not be masked at all. Diffuse irradiation, on the other hand, will be determined by the proportion of sky which is obscured by rows of panels in all directions. We assume diffuse irradiation is isotropic with uniform distribution in all directions and ignore the effect of ground-reflected irradiance. Similarly, we assume the AVS site has flat ground while calculating ground horizontal irradiation.

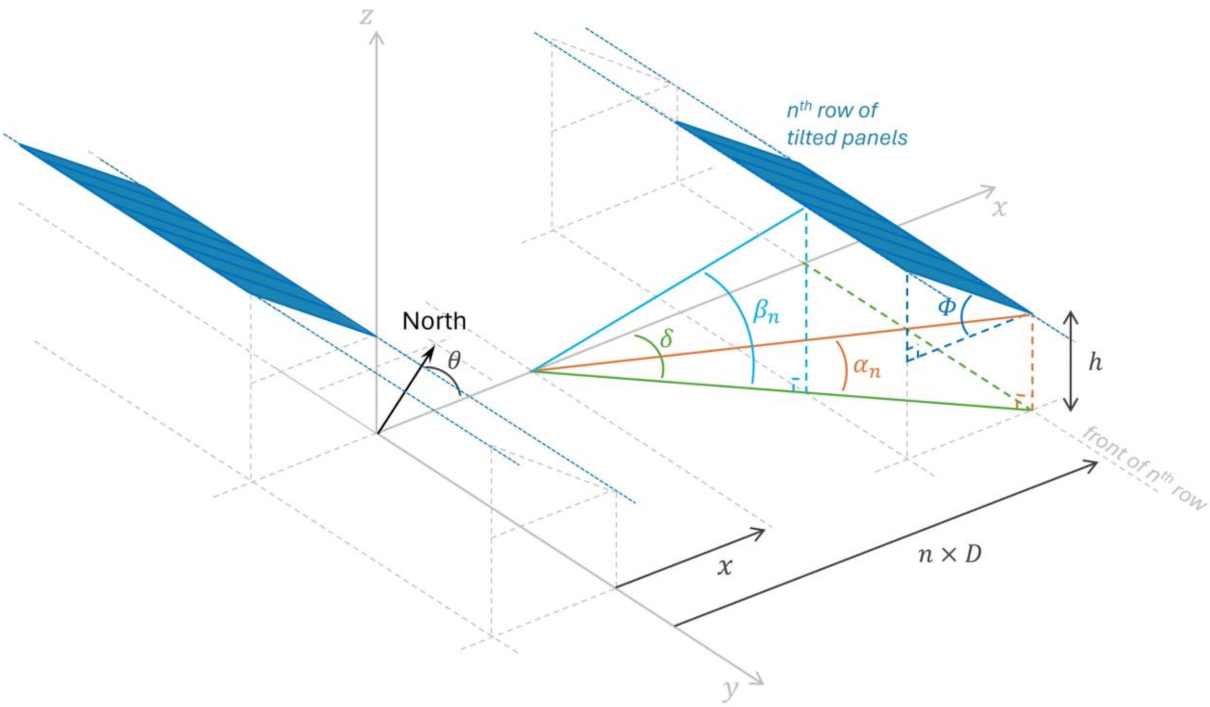

Figure 1. *Schematic representation of sky visibility at any ground position x considering the masking effect of the n^{th} row of solar panels.*

For a given ground position, shading can occur because of all rows of panels in both directions, with the more distant rows having diminishing impact. It is straightforward to show that shading can be accurately calculated if a sufficient number, N, of the closest rows only are considered. Since rows repeat at a regular spacing, we need only to determine shading and insolation at all positions between two adjacent rows, caused by N rows in either direction. Consider the position on a perpendicular line between two adjacent rows, a distance x from the front of the first row. The impact of the n^{th} row on shading at position x is then calculated by determining the angle subtended by that row of panels (thus obscuring the sky) for all horizontal angles of rotation, δ, from this perpendicular line. For any horizontal angle δ, the sky segment is obscured by n^{th} row of solar panels if the altitude angle of the sky region lies between α_n and β_n, which is determined by using Equation (1) and Equation (2).

$$\alpha_n = tan^{-1}\frac{h.cos\delta}{n.D - x} \tag{1}$$

$$\beta_n = tan^{-1}\frac{(h + l.sin\,\phi)\,cos\,\delta}{n.D - x - l.cos\,\phi} \tag{2}$$

where, α_n and β_n are angles made by the lower edge and upper edge of the n^{th} row of solar panels, respectively, with the ground at position x.

At position x, the fraction of the sky hemisphere that is unobstructed by solar panels is then determined using [16], which is referred to as the clear sky fraction (CSF_x). Similarly, the sun position algorithm [17] is used to obtain solar azimuth angle (S_{Az}) and altitude angle (S_{Al}) at any time (yyyy-mm-dd-hr-mm-ss). At each time step, the sky visibility factor at position x (SVF_x) is determined based on whether the sky segment is obscured by any of the rows of the solar panel in the direction of the solar azimuth angle. Consequently, the global horizontal irradiation at position x (GHI_x), is determined as:

$$GHI_x = CSF_x.DHI + SVF_x.DNI.cos(90° - S_{Al}) \tag{3}$$

where DHI and DNI are diffuse horizontal irradiance and direct normal irradiation, respectively, received at the AVS location, for open-field conditions.

2.2 Clustering Algorithm

The k-medoids function in MATLAB® [18] was used to group the insolation profiles observed at ground positions within AVS layouts into a ‘k’ cluster based on the minimum Euclidean distance between each insolation profile and centroids of 'k' clusters. The number of clusters (k) into which insolation profiles are divided was first selected using the elbow method, such that these groups of insolation profiles corresponded to 90% of the explained variance. The K-medoid clustering was then performed with 100 repetitions to ensure that the selection of centroids of clusters resulted in the minimum total sum of distances.

2.3 Agricultural Production, Energy Generation and Land Productivity under AVS

Following the clustering of insolation profiles, the insolation profile of the centroid of each of the 'k' clusters can be used to represent the heterogeneous insolation distribution observed across the ground within AVS. As many agricultural systems models only use a single value for daily solar irradiation, each of these 'k' insolation profiles can be set as an input to determine daily agricultural production under each insolation cluster (y_k). For every AVS layout, the clustering algorithm also provides information about how many ground positions are grouped under each of the 'k' clusters. This information can be used to determine the percentage of land area occupied by each cluster within each AVS layout (a_k). Hence, the agricultural production of each AVS layout is then determined as follows:

$$Agricultural\ Production_{AVS} = \sum_{1}^{k} a_k . y_k \tag{4}$$

Electrical energy yield for any AVS layout can be determined by modeling PV systems using any conventional PV system model. Consequently, the land equivalent ratio achieved by each AVS layout is computed as:

$$LER = \frac{Energy\ Generation_{AVS}}{Energy\ Generation_{max}} + \frac{Agricultural\ Production_{AVS}}{Agricultural\ Production_{open-field}} \tag{5}$$

where *Energy Generation$_{max}$* is the electrical energy generated by standalone ground-mounted PV systems, which aims to maximize both energy yield (kWh/yr) and land utilization (kWh/ha), *Agricultural Production$_{open\text{-}field}$* is agricultural yield achieved through standalone agri-food agriculture, and *Agricultural Production$_{AVS}$ and Energy_Generation$_{AVS}$* are agricultural production and electrical energy generated by each AVS layout, respectively.

2.4 Parameters Selected for Case Study

We illustrate our approach using a case study to demonstrate its effectiveness in modelling agricultural production in AVS using point based agricultural model. We also illustrate how the method can be used to determine an optimal AVS layout, for the case study location near Hobart, Australia (Lat: -42.9° N, Long: 147.32° E). The Typical Meteorological Year (TMY) weather data for this location was obtained from the National Renewable Energy Laboratory's (NREL) National Solar Radiation Data Base (NSRDB) [19]. The weather data provided hourly solar radiation data of direct normal irradiance (DNI) (W/m^2) and diffuse horizontal irradiance (DHI) (W/m^2), temperature (°C), dew Point (°C), surface albedo, pressure (mbar), wind speed (m/s), and relative humidity (%). TMY data is suitable for representative single-year simulations, since it accurately represents the average long-term local weather conditions while still reflecting a range of typical weather phenomena that have occurred, based on historical observations over numerous years at that location.

For insolation modelling and determining GHI at ground positions for different AVS layouts, we considered North facing solar panels of length 2 m with the lower edge of each row of tilted panels being placed 4 m above ground level. The ground was assumed flat and insolation calculations were performed at 20 equally spaced positions between adjacent rows, with shading impacts calculated for 8 rows of panels in either direction. In total, 81 different AVS layouts were considered, by varying both row-spacing (from 4 m to 20 m at 2 m intervals) and solar panel tilt angle (between 0° and 40° in 5° intervals).

GrassGro (version 3.4.3) [20] was adopted for this case study demonstration to determine pasture biomass yield at areas within AVS receiving heterogenous insolation distribution. GrassGro computes pasture production, pasture growth rate, ground cover and many other factors relating to pasture and livestock production systems [21]. As GrassGro requires daily solar radiation as an input parameter, the insolation modelling calculations performed at the 15-minute time step were summed up to obtain daily ground surface insolation and provided as an input parameter to GrassGro. For simplicity in model design and to enable a clearer assessment of the impact of shading caused by solar panels on growth of vegetation, this study models an ungrazed farming enterprise. Pasture species comprised of perennial ryegrass (*Lolium perenne*) and Leura subterranean clover (*Trifolium subterraneum* subsp. subterraneum cv. Leura), which are commonly established pasture species in Tasmania. We assumed pastures were cut to produce hay whenever pasture production exceeded 2,500 kg DM/ha.

The System Advisor Model (SAM®) version 2022.11.21 [11] was used to model the electricity production of grid-connected PV systems. The solar panel selected for this study was 'LG400N2C-A5', which has dimensions of 2 m x 1 m. The selected inverter was 'WSTECH

Gmbh: APS800-ES-1-440-5[440V]'. Each row of solar panel consisted of 500 solar panels, and in total there were 16 rows of solar panels (aligning with 8 rows in either direction (Figure 1) considered for insolation modelling in subsection 2.1). The total installed capacity was 3.2 MW_{dc}, which comprised 8,000 solar panels. The row space was selected by adjusting ground cover ratio parameter in SAM. The annual electrical energy generated by the PV system was simulated by providing TMY weather data to SAM as an input, along with parameters such as tilt angle of solar panels ϕ and their azimuth angle θ.

3. Results & Discussion

Figure 2 illustrates the annual insolation observed at 20 ground positions for the 81 AVS layouts and shows a trend of increase in annual insolation received at ground positions as the row space increases. The presence of solar panels causes a heterogeneous insolation distribution across the ground surface in AVS, even when only observing the annualized insolation. This non-uniformity is more pronounced when observing daily or hourly insolation profiles across the field (not shown here).

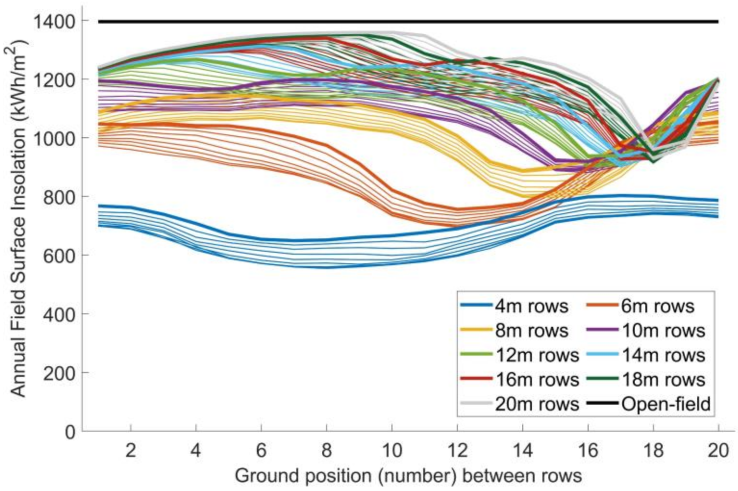

Figure 2. *Annual insolation observed at 20 ground positions in the row space for 81 AVS layouts compared with the open field. For each row space shown in the legend, tilt angle was varied from 0^0 to 40^0 at step size of 5^0.*

3.1 Clustering of Insolation Profiles

For each of the 81 AVS layouts, daily insolation received at 20 ground positions for 365 days in a year was calculated, which produced 1620 insolation profiles. The clustering algorithm grouped these 1620 insolation profiles into 19 insolation clusters. Annual insolation observed at 20 ground positions for four randomly selected AVS layouts out of 81 layouts is shown in *Figure 3*. As illustrated by the arrows and subplots in *Figure 3*, similar daily insolation profiles observed at various ground positions across different AVS layouts are grouped into the same insolation cluster (one of 19 clusters). For example (*Figure 3*), ground positions 13, 14, and 15 in AVS layout 16, as well as ground positions 15 and 16 in layout 25, are grouped under cluster 5 because they receive similar daily insolation profiles, distinct from those of other clusters (18 and 19). It should be noted that, although two different ground positions for different layouts may have almost identical annual insolation (as shown in the primary plot of *Figure 3*), significant differences in the daily insolation across the year lead to them being grouped into different insolation clusters. The clustering approach also allows us to determine the proportion of land area occupied by each cluster (via information on how many of the 20 ground positions are grouped under each of 19 insolation clusters) for each of the 81 AVS layouts. This is illustrated in *Figure 4*, which shows that more land area within the AVS site receive higher insolation levels when row space is increased.

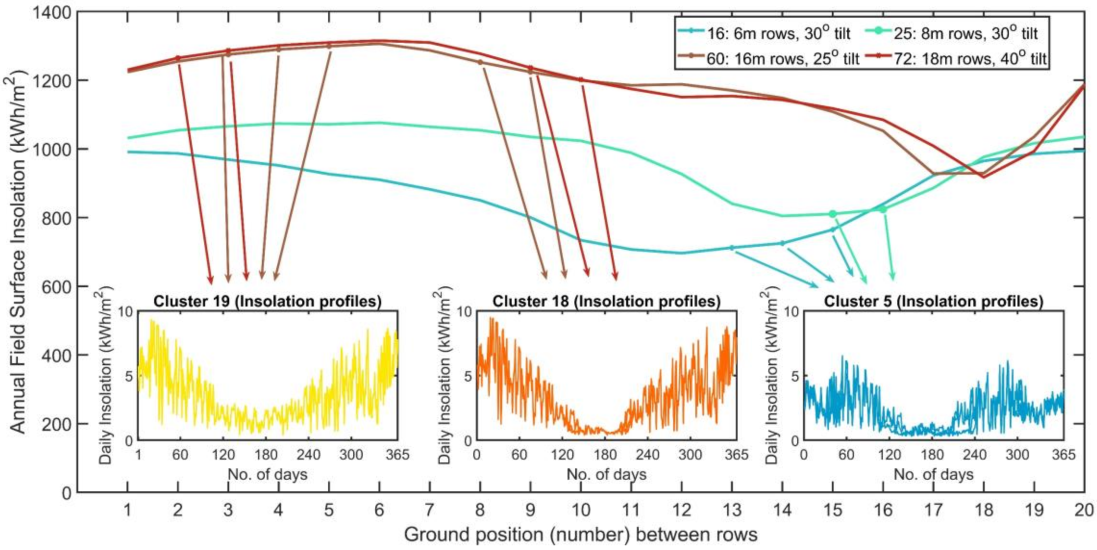

Figure 3. *An illustration of clustering of insolation profiles observed at 20 ground position of various AVS layouts. The arrows directed to the subplots indicate that similar daily insolation profiles received at various ground positions for different AVS layouts were grouped into the same cluster group.*

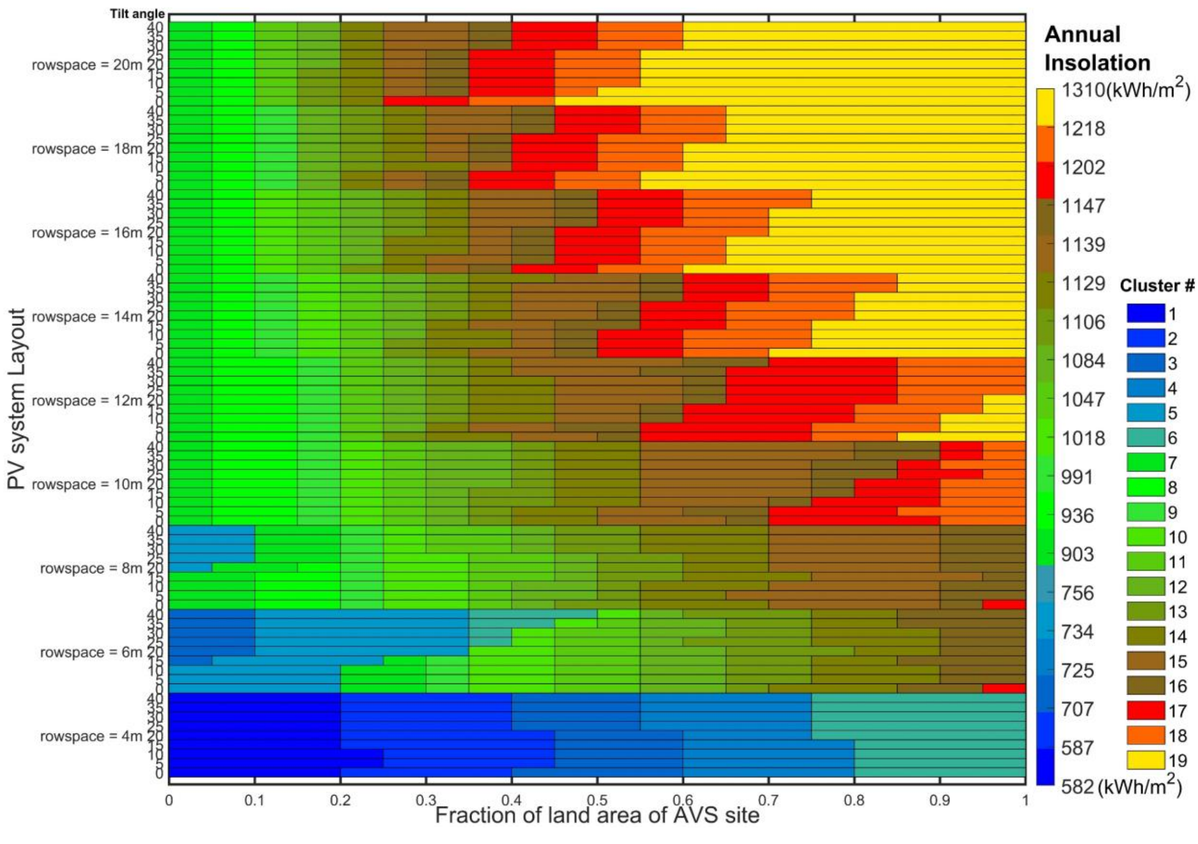

Figure 4. *The proportion of land occupied by insolation clusters for each of the 81 AVS layouts. The clusters are labelled according to the annual insolation levels received by them. Cluster 1 indicates ground positions receiving the lowest annual insolation of 582 kWh/m², while cluster 19 indicates ground positions receiving the highest insolation of 1310 kW/m² in AVS.*

Figure 5 shows the simulated pasture growth rate in open-field and at ground positions within AVS, with the latter receiving one of 19 distinct daily insolation profiles represented by the centroid of its respective cluster. The growth rates within AVS (for the 19 insolation profiles) are lower than those in the open field for most of the year (February to October), except during late spring and summer (November to December), as illustrated in *Figure 5*. Notably, a sharp decline in growth rates is observed between spring (October-November) and summer (January-February), primarily due to generally unfavorable conditions for pasture growth in summer. In spring, soil moisture is high, temperatures are optimal for growth (20-30°C), and radiation levels are abundant, all of which support robust pasture growth. By contrast, in summer, temperatures are often supraoptimal (causing plant senescence), soil moisture is low, and hot dry air at ground level typically extracts more water from leaves than roots are able to supply from available soil moisture, all of which hinder pasture growth. The reduction in solar radiation in AVS farms limits pasture growth for most of the year, with some parts of the field (generally field positions of AVS with closely placed solar panels) experiencing considerably lower growth rates for much of the year owing to severe insolation reduction. In contrast, the total annual pasture yield for clusters 17 and 19 is greater than for open field conditions. The increase in yield for these clusters, characterized by an overall late-season boom in pasture production in AVS, can be attributed to a decrease in evapotranspiration losses during the hotter and drier months of the year. The reduction in evapotranspiration helps alleviate plant stress related to water deficit when vapor pressure deficit rises and rainfall declines. This impact is further illustrated in *Figure 6*, which plots monthly pasture growth rates for each AVS layout (calculated from cluster growth rates and cluster composition (Figure 4) of each layout), with higher pasture growth rates being achieved during the late spring and summer for all 81 AVS layouts. Graham et al. report a similar finding, where late season floral abundance was observed in AVS caused by partial shading conditions created by the solar panels, highlighting benefits for livestock producers in water-limited regions [22].

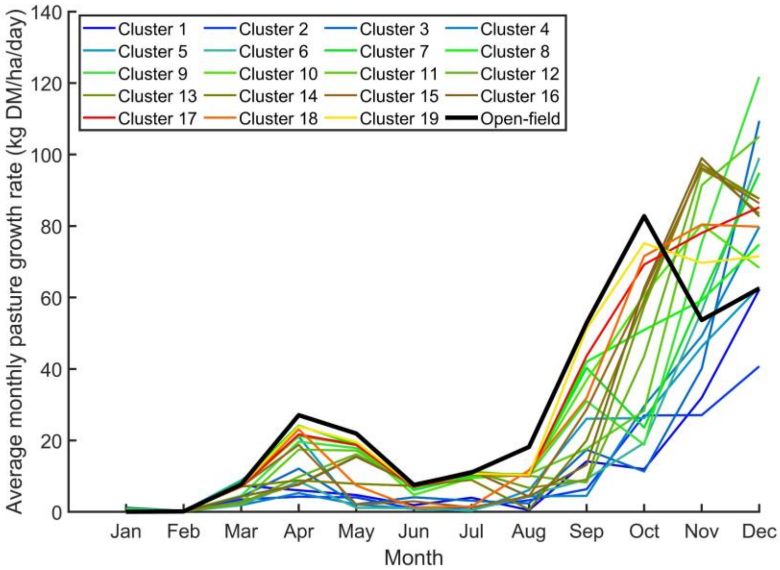

***Figure 5**. Comparison between monthly pasture growth rate in open field conditions and growth rate within AVS for the insolation profile of each cluster.*

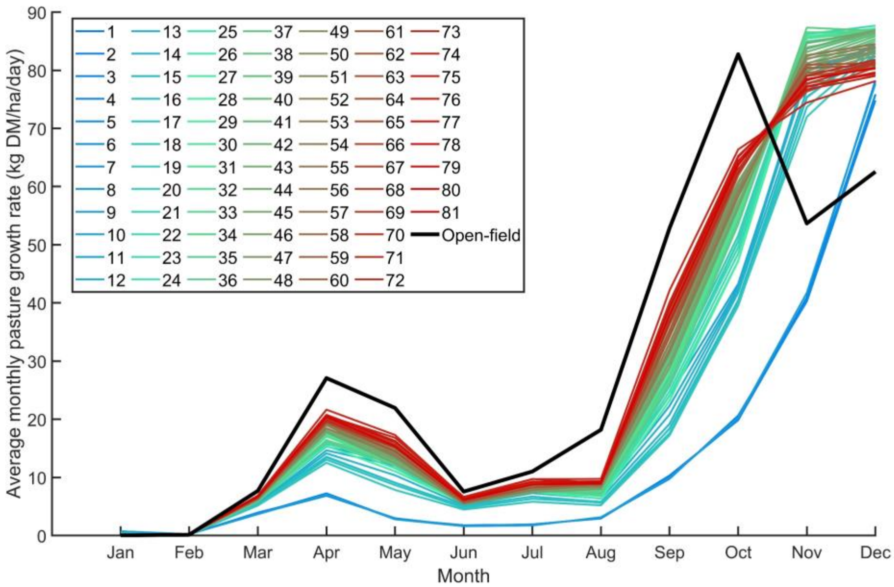

Figure 6. *Comparison of monthly pasture growth rate in open field conditions and growth rate in AVS layouts. Here, AVS layouts 1-9, 10-18, 19-27, 28-36, 37-45, 46-54, 55-63, 64-72, 73-81 represent AVS layouts with row spaces 4 m, 6 m, 8 m, 10 m, 12 m, 14 m, 16 m, 18 m, and 20 m, respectively with tilt angles varied among them from 0° to 40° varied at steps of 5°.*

3.2 Optimization of AVS Layout

Figure 7 shows the calculated AVS to open-field pasture production ratio, the AVS to conventional PV system energy generation ratio and the LER for each of the 81 investigated AVS layouts. The energy generated per hectare for both ground-mounted PV systems and AVS layout case 6 (rows of 4 m and tilt angle of 25°) was 1,178 MW/ha. As row spacing is increased from 4 m, the energy yield per hectare decreases proportionally while pasture production increases, approaching the open-field pasture yield of 10.5 t DM/ha. With a maximum LER of 1.49, the optimal PV system layout comprised of 4 m rows with panels tilted at 25°. However, this AVS layout severely reduced agricultural production, to about half that for the open field, which may run counter to an agricultural practitioner's objectives. By increasing row space to 6 m and with panels tilted at 15°, pasture production could achieve 80% of yield for open-field farming, but with a comparable overall LER of 1.47. Similarly, the AVS layout with highest LER (LER = 1.4) that still ensures greater than 90% of agricultural output compared with open-field production consisted of 8 m rows with tilt angle of 15°. All three of these AVS layouts increase land productivity considerably compared to separate PV electricity generation and pasture production systems.

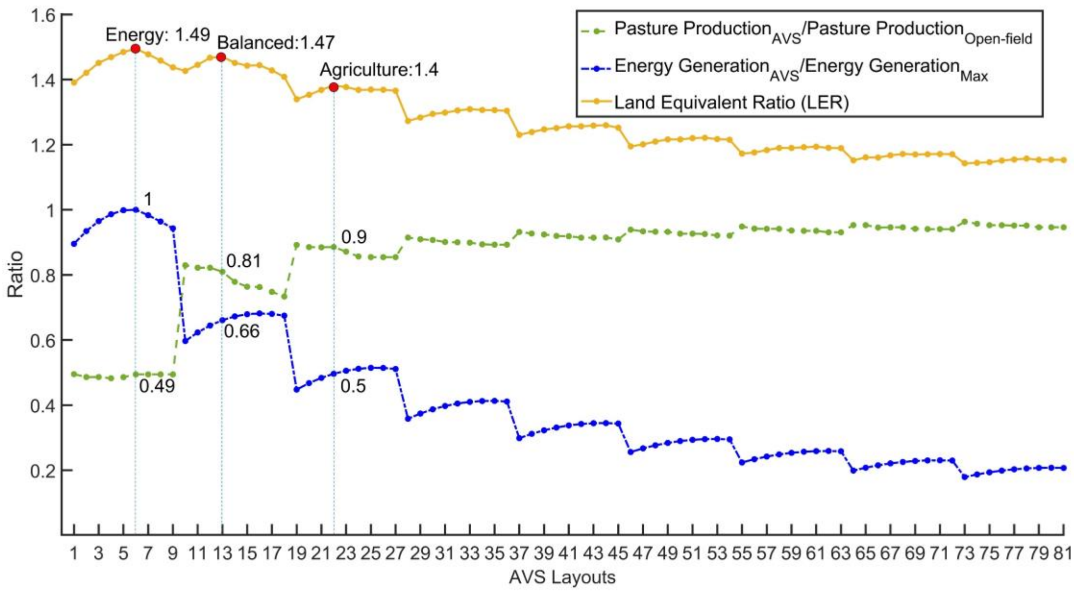

Figure 7. *Land Equivalent Ratio of AVS Layouts.*

4. Conclusion

Here, we exemplify a novel method for incorporating outputs from point-based agricultural systems models to determine plant growth characteristics in AVS, accounting for heterogeneous insolation within agrivoltaic farms. Our approach enables efficient optimization of AVS layouts to meet any given electrical energy and pasture biomass production objective by requiring upfront evaluation of pasture biomass yield for a small number of clustered insolation profiles. Our case study showed that the optimal PV system layout depends on the optimization objective. A PV layout with 4 m rows and 25° tilted panels, for example, can achieve maximum land equivalent ratio (LER). However, this AVS layout severely reduces pasture biomass yield. Thus, a more appropriate design that balances agricultural production and energy generation with comparable LER can be achieved by using a PV layout comprising of 6 m rows and panels titled at 15° at the location studied.

Our method can be readily adapted to elicit optimal AVS layout for any location, assuming appropriate weather and soil data are available. We suggest that future studies should consider varying orientation and mounting height of panels, along with tilt angle and row spacing, as well as non-tracking and tracking PV systems. The approach can be used to determine optimal AVS layouts for various optimization objectives, such as maximizing land use productivity, maintaining threshold levels of electricity and/or agricultural yield, or balancing priorities between economic, environmental and/or social license aspirations.

Data availability statement

The data will be available from the corresponding author upon request.

Author contributions

GP: Conceptualization, Methodology, Software, Data curation, Visualization, Writing- original draft. SL: Conceptualization, Supervision, Project administration, Writing – review & editing. EF: Conceptualization, Methodology, Software, Visualization, Supervision, Writing – review & editing. MTH: Conceptualization, Software, Supervision, Writing – review & editing.

Competing interests

The authors declare that they have no competing interests.

References

[1] C. Dupraz, H. Marrou, G. Talbot, L. Dufour, A. Nogier, Y. Ferard, "Combining solar photovoltaic panels and food crops for optimising land use: Towards new agrivoltaic schemes," Renewable Energy, vol. 36, no. 10, pp. 2725-2732, 2011/10/01/ 2011, doi: https://doi.org/10.1016/j.renene.2011.03.005.

[2] I. A. Ramos-Fuentes, Y. Elamri, B. Cheviron, C. Dejean, G. Belaud, D. Fumey, "Effects of shade and deficit irrigation on maize growth and development in fixed and dynamic AgriVoltaic systems," Agricultural Water Management, vol. 280, p. 108187, 2023, doi: https://doi.org/10.1016/j.agwat.2023.108187.

[3] S. Amaducci, X. Yin, M. Colauzzi, "Agrivoltaic systems to optimise land use for electric energy production," Applied Energy, vol. 220, pp. 545-561, 2018/06/15/ 2018, doi: https://doi.org/10.1016/j.apenergy.2018.03.081.

[4] R. I. Cuppari, C. W. Higgins, G. W. Characklis, "Agrivoltaics and weather risk: A diversification strategy for landowners," Applied Energy, vol. 291, p. 116809, 2021, doi: https://doi.org/10.1016/j.apenergy.2021.116809.

[5] R. Handler, J. M. Pearce, "Greener sheep: Life cycle analysis of integrated sheep agrivoltaic systems," Cleaner Energy Systems, vol. 3, p. 100036, 2022, doi: https://doi.org/10.1016/j.cles.2022.100036.

[6] A. S. C. Maia, E. de Andrade Culhari, V. d. F. C. Fonsêca, H. F. M. Milan, K. G. Gebremedhin, "Photovoltaic panels as shading resources for livestock," Journal of Cleaner Production, vol. 258, p. 120551, 2020, doi: https://doi.org/10.1016/j.jclepro.2020.120551.

[7] M. Laub, L. Pataczek, A. Feuerbacher, S. Zikeli, P. Högy, "Contrasting yield responses at varying levels of shade suggest different suitability of crops for dual land-use systems: a meta-analysis," Agronomy for Sustainable Development, vol. 42, no. 3, p. 51, 2022, doi: https://doi.org/10.1007/s13593-022-00783-7.

[8] S. Gorjian, E. Bousi, Ö. E. Özdemir, M. Trommsdorff, N. M. Kumar, A. Anand, K. Kant, S. S. Chopra, "Progress and challenges of crop production and electricity generation in agrivoltaic systems using semi-transparent photovoltaic technology," Renewable and Sustainable Energy Reviews, vol. 158, p. 112126, 2022, doi: https://doi.org/10.1016/j.rser.2022.112126.

[9] C. Toledo, A. Scognamiglio, "Agrivoltaic systems design and assessment: A critical review, and a descriptive model towards a sustainable landscape vision (three-dimensional agrivoltaic patterns)," Sustainability, vol. 13, no. 12, p. 6871, 2021, doi: https://doi.org/10.3390/su13126871.

[10] H. Dinesh, J. M. Pearce, "The potential of agrivoltaic systems," Renewable and Sustainable Energy Reviews, vol. 54, pp. 299-308, 2016/02/01/ 2016, doi: https://doi.org/10.1016/j.rser.2015.10.024.

[11] *System Advisor Model (SAM) Version 2022.11.21*. National Renewable Energy Laboratory. Golden, CO. Accessed: 2-March 2023. [Online]. Available: https://sam.nrel.gov/

[12] B. Valle, T. Simonneau, F. Sourd, P. Pechier, P. Hamard, T. Frisson, M. Ryckewaert, A. Christophe, "Increasing the total productivity of a land by combining mobile photovoltaic panels and food crops," Applied energy, vol. 206, pp. 1495-1507, 2017.

[13] S. Kim, Y. Kim, Y. On, J. So, C.-Y. Yoon, S. Kim, "Hybrid performance modeling of an agrophotovoltaic system in South Korea," Energies, vol. 15, no. 18, p. 6512, 2022, doi: https://doi.org/10.3390/en15186512.

[14] P. E. Campana, B. Stridh, S. Amaducci, M. Colauzzi, "Optimisation of vertically mounted agrivoltaic systems," Journal of Cleaner Production, vol. 325, p. 129091, 2021/11/20/ 2021, doi: https://doi.org/10.1016/j.jclepro.2021.129091.

[15] M. S. Ahmed, M. R. Khan, A. Haque, M. R. Khan, "Agrivoltaics analysis in a techno-economic framework: Understanding why agrivoltaics on rice will always be profitable," Applied Energy, vol. 323, p. 119560, 2022, doi: https://doi.org/10.1016/j.apenergy.2022.119560.
[16] M. Silva, J. J. Roberts, P. O. Prado, "Calculation of the shading factors for solar modules with matlab," Energies, vol. 14, no. 15, p. 4713, 2021, doi: https://doi.org/10.3390/en14154713.
[17] I. Reda, A. Andreas, "Solar position algorithm for solar radiation applications," Solar energy, vol. 76, no. 5, pp. 577-589, 2004, doi: https://doi.org/10.1016/j.solener.2003.12.003.
[18] The MathWorks Inc., MATLAB version: 9.11 (R2021b), Accessed: January 14, 2023 2021. [Online]. Available: https://www.mathworks.com.
[19] National Renewable Energy Laboratory (NREL). NSRDB: National Solar Radiation Database. [Online]. Available: https://nsrdb.nrel.gov/data-viewer
[20] *GrassGro®*, Commonwealth Scientific and Industrial Research Organisation (CSIRO). [Online]. Available: https://grazplan.csiro.au/grassgro/.
[21] F. Bilotto, K. M. Christie-Whitehead, B. Malcolm, M. T. Harrison, "Carbon, cash, cattle and the climate crisis," Sustainability Science, pp. 1-17, 2023, doi: https://doi.org/10.1007/s11625-023-01323-2.
[22] M. Graham, S. Ates, A. P. Melathopoulos, A. R. Moldenke, S. J. DeBano, L. R. Best, C. W. Higgins, "Partial shading by solar panels delays bloom, increases floral abundance during the late-season for pollinators in a dryland, agrivoltaic ecosystem," Scientific reports, vol. 11, no. 1, pp. 1-13, 2021, doi: https://doi.org/10.1038/s41598-021-86756-4.